RSC Advances

ROYAL SOCIETY OF CHEMISTRY

www.rsc.org/advances

Cite this: DOI: 10.1039/c0xx00000x

www.rsc.org/loc

PAPER

Photobleaching induced time-dependent light emission from dye-doped polymer nanofibers

Weina Zhang, Juan Li, Hao Chen, and Baojun Li*

Received (in XXX, XXX) Xth XXXXXXXXX 20XX, Accepted Xth XXXXXXXXX 20XX

DOI: 10.1039/b000000x

Photobleaching has a great impact on the light emission of dye-doped polymer nanofibers. Here, we report photobleaching induced time-dependent light emission along polymer nanofibers doped with Coumarin-6 and Lumogen-F-Red-305 via waveguiding excitation at a wavelength of 473 nm. A nanofiber with a diameter of 450 nm was observed with emission color changing from green to red after 57 minutes excitation with an optical power of 4 μW at 473 nm wavelength. Spectrum analysis indicates that the major emission peaks were shift from 492 to 590 nm. The photoluminescence was further found changing at different rates along the nanofiber. The experiment infers that the light emission is a function of both time and position along the nanofiber.

Introduction

Light emission from one-dimensional nanostructures like nanofibers or nanowires, are of great importance for nanophotonic integration. Especially, dye-doped polymer nanofibers with the advantage of high efficient light emission have attracted plenty of attention as active nanowaveguides[1-3], optically pumped lasers[4,5], and white light emitters[6-9]. These components are demanded to work over a long term under continuous excitation. It is known that fluorescent dyes suffer from a disadvantage of photobleaching which induces photoluminescence (PL) decay as a function of time[10-12], having a great impact on the photostability of the dye-doped polymer nanofibers. Hence, investigation on photobleaching induced time-dependent light emission property of the dye-doped polymer nanofibers is necessary and desired. Fortunately, experiments have already been demonstrated that, PL intensity from polymer nanofibers doped with a single dye exhibits an exponential decay as a function of time under continuous irradiation due to the photobleaching of the doped dye molecules[13-14]. On the other hand, by doping different dyes, polymer nanofibers can be fabricated with a broad emission such as white light emitters. However, the broad PL spectrum changes versus time due to diverse photobleaching rates of different doped dyes. Therefore, photobleaching causes a larger impact on polymer nanofibers doped with different dyes. Furthermore, photobleaching is dependent on the intensity of the excitation light[10,15,16], which attenuates when guided along the polymer nanofibers[17-19]. This indicates that PL will decay with different photobleaching rates at different positions along the polymer nanofibers. Therefore, two different dyes codoped photobleaching in a single nanofiber is a very important issue to be studied. Via waveguiding excitation, it is able to couple excitation light into polymer nanofibers and investigate time-dependent light emission at different positions along the polymer nanofibers doped with different dyes. Here we report photobleaching induced time-dependent light emission at different positions along dual-dye-doped polymer nanofibers via waveguiding excitation (optical fiber), which is more beneficial for photonic integration in comparison with the focusing excitation (microscope objective) used in previously reported studies[13]. Both emission color and spectra of the emitted light were found changing with different rates at different positions along the polymer nanofibers. The study is important and is beneficial in improving the bleaching of the dye doped fibers. For example, the study would be helpful for obtaining stable white light emitters.

Experiment

Poly(methyl methacrylate) (PMMA), with a refractive index of 1.49, was chosen as a matrix material for nanofiber fabrication, considering its transmission of over 80% at a broad wavelength range of 350 to 1600 nm, which covers all visible lights. Coumarin 6 (C6) and Lumogen F Red 305 (LR305) were chosen as dopants with very different photobleaching rates at a wavelength of 473 nm, which served as the excitation wavelength in the experiment. Polymer nanofibers were fabricated via a directly drawing method[20]. First, 7 g of PMMA was dissolved in 25 ml acetone at 25°C to form a solution with an appropriate viscosity for drawing. Second, C6 (purchased from J&K Chemical Co. Ltd.) and LR305 (from BASF Co. Ltd.) were dissolved together in acetone with a mass ratio of C6 : LR305 = 1 : 1 and a concentration of 0.1 wt%. Third, the dye-acetone solution was added into the prepared PMMA-acetone solution, forming a viscous blend with a mass ratio of C6 or LR305 to PMMA = 1 : 3500. Then, the blend was kept under thoroughly magnetic stirring at 25°C for 3 hours to guarantee uniformity of doping. Fourth, a silica optical fiber taper with a tip diameter of 5 μm was immersed into the sample solution so that the blend was

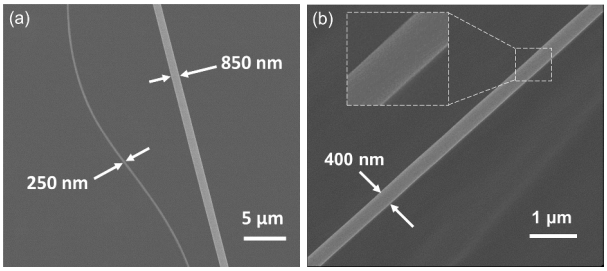

Fig. 1 SEM images of C6-LR305-codoped polymer nanofibers. (a) Two nanofibers with respective diameters of 250 and 850 nm. (b) A representative nanofiber with a diameter of 400 nm. Inset is the close-up view of the nanofiber.

attached to the tip. As soon as the taper was pulled out at a speed of approximately 1 m/s, the viscous blend on the tip extended into a long wire because of the rapid evaporation of acetone. As a result, a dye-doped polymer nanofiber was obtained. The diameters and lengths of the nanofibers can be controlled by changing the viscosity of the sample solution and the drawing speed. For instance, smaller diameter nanofibers can be drawn with a less viscous solution at a faster drawing speed. Figure 1(a) shows a typical scanning electron microscope (SEM) image of as-fabricated C6-LR305-codoped polymer nanofibers with respective diameters of 250 and 850 nm. Figure 1(b) shows a representative 400 nm diameter nanofiber. It can be seen from the close-up view in the inset of Fig. 1(b), the nanofiber exhibits a good uniformity and sidewall smoothness with a maximum diameter variation $\Delta D \approx 20$ nm over a length $L = 700$ nm, indicating there is no obvious defect on the surface of the nanofibe.

The waveguiding excitation and spectral measurement have been performed by laying the nanofibers on an MgF_2 substrate under a spectrophotometer (CRAIC 20) as schematically shown in Fig. 2(a). The refractive index of MgF_2 (1.39) is lower than that of PMMA (1.49), ensuring a tight light confinement in the nanofiber and little light leakage to the substrate. The nanofiber was excited via waveguiding excitation at the wavelength of 473 nm which was coupled by a tapered silica fiber tip. PL was collected by a spectrophotometer and a CCD. Efficient coupling was achieved by placing the fiber taper and the nanofiber in close contact forming a junction. Due to van der Waals and electrostatic attraction, the junction between the nanofiber and the fiber taper can be maintained[20]. Figure 2(b) shows that white light from a halogen lamp (Yokogawa AQ4305) was coupled into the nanofiber by tapered fiber 1. The output light from the nanofiber was collected by a spectrometer (Ocean Optics, USB2000+) via tapered fiber 2. The excitation light from the 473-nm laser was output from the fiber 3 whose end was flat.

Results and discussion

The C6-LR305-codoped polymer nanofiber was firstly excited by the 473 nm blue light output from the fiber 3 (see Fig. 2(b)) with an intensity of $I_{ex} = 1.3\times10^6$ Wm^{-2} (excitation power $P_{ex} = 800$ μW, light spot: 600 μm^2) for a certain time t. The actual optical power P_{in} coupled into the codoped polymer nanofiber was estimated to be 1.5 μW (See Figure S1 in the Supplementary Information). Then the blue light was turned off followed by turned on the white light and scanning the absorbance. Figure 3(a) shows the measured absorbance at different excitation time. It can

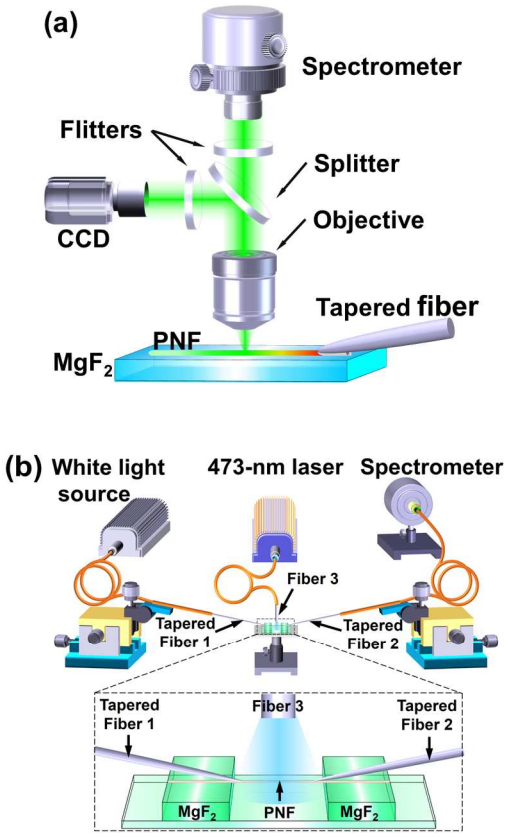

Fig. 2 Schematic experimental setup for (a) waveguiding excitation and PL spectrum measurement and (b) absorbance measurement of polymer nanofiber (PNF).

be seen that, without excitation ($t = 0$, red curve), there are three absorption peaks at 453, 530, and 577 nm wavelengths, which can be ascribed to co-doped dyes. Especially, a high absorbance of 0.81 was found at the scanning wavelength of 473 nm. The absorption peaks decreases with the increase of excitation time t of the blue light. This is owing to photobleaching. After 100 minutes excitation, the absorption peak at 453 nm decreases as much as 75%, while at 530 and 577 nm only decrease 5% and 12%, respectively. Especially, absorbance at 473 nm decreased 76.5% from 0.81 to 0.19, indicating reducing consumption of the excitation power. Figure 3(b) shows the re-plotted absorbance at 453, 473, 530, and 577 nm as a function of excitation time t. It can be seen that, with continuous excitation, the absorbance at 453 nm (green-dotted curve) and 473 nm (blue-dotted curve) decreases quickly, while the absorbance at 530 nm (pink-dotted curve) and 577 nm (red-dotted curve) stayed relatively stable. The decrease of absorbance with increasing excitation time shown in Figs. 3(a) and 3(b) is owing to photobleaching caused by photooxidation, the collision between the fluorophores molecules and the interaction between the excitation photons and fluorophores molecules in excited states. The fluorescence emission occurs when the electrons in the first excited singlet state return back to the ground state under the radiation of laser source. However, the photooxidation, reaction of dye to dye molecules and dye to incident photons will lead to an irreversible

conversion of fluorescent molecules into a nonfluorescent entity, which decreases the number of fluorophores participating in the emitting fluorescence. As a result, the absorbance of C6-LR305-codoped nanofibers reduces as a function of time. In addition, the absorbance is also related to the excitation power. To investigate the temporal behavior of absorbance with different excitation powers P_{ex}, an additional experiment has been performed. The result shows that, with increasing P_{ex}, the absorbance decreases more quickly and the photobleaching is more obvious, which is consistent with the reported results[15,16]. More details and an additional Figure S2 have been added in the Supplementary Information.

For comparison, C6-doped and LR305-doped nanofibers were also prepared with the same C6 and LR305 contents as those in the C6-LR305-codoped nanofiber. Figure 3(c) shows a comparison of the absorbance between the C6-LR305-codoped, C6-doped, and LR305-doped nanofibers. The absorbance curve of the C6-LR305-codoped nanofiber (black curve) fits well with the sum (magenta-dashed curve) of the absorbance of C6-doped (green curve) and LR305-doped (red curve) nanofibers, which indicates that the codoping only influences the individual absorbance of either C6 or LR305 molecules. In the wavelength range of 350 to 700 nm, the C6-doped nanofiber exhibits an absorption peak at 456 nm. The absorption peaks at 442, 530, and 577 nm are ascribed to LR305-doped nanofiber. Furthermore, C6 absorbs much stronger than that of LR305 at around 453 nm but is transparent at 577 nm, where LR305 exhibits an absorption peak instead. Especially, the absorbance (0.76) of the C6-doped nanofiber at 473 nm is approximately 25 times larger than that of the LR305-doped nanofiber (0.03), which indicates that more than 96% of excitation power was absorbed by the C6. Thus, it can be concluded from Fig. 3(c) that, the absorption peak of the C6-LR305-codoped nanofiber at 453 nm is mainly attributed to the C6, while the peak at 577 nm is attributed to the LR305.

By considering Figs. 3(a)–(c), as time goes on, the stability of absorbance at 577 nm infers the stability of the LR305 molecules,

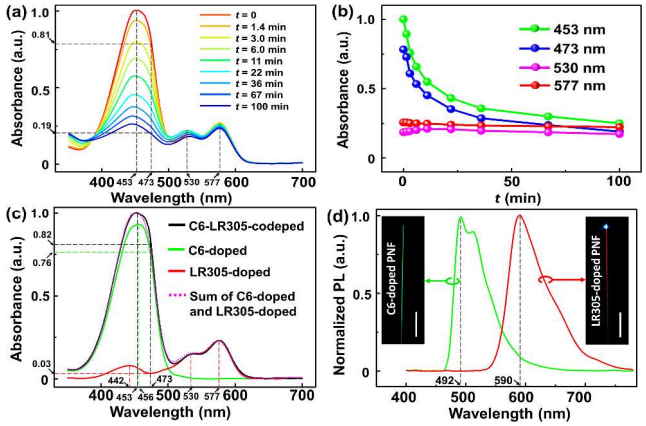

Fig. 3 (a) Absorbance of C6-LR305-codoped polymer nanofiber after excitation by 473-nm blue light. Different curves represent different excitation time. (b) Absorbance at 453, 473, 530, and 577 nm as a function of excitation time *t*, which were picked from the absorbance curves in (a). (c) Absorbance of C6-doped (green curve), LR305-doped (red curve), C6-LR305-codoped (black curve) nanofibers, and the sum (magenta dash curve) of the absorbance of C6-doped and LR305-doped nanofibers. (d) Normalized PL of LR305-doped polymer nanofiber (PNF) (red curve) and C6-doped (green curve) PNF. Insets: microscope images of the C6-doped PNF and the LR305-doped PNF with a diameter of ~ 600 nm. Scale bar: 50 μm.

and the decreasing absorbance at 453 nm infers the photobleaching of the C6 molecules. Figure 3(d), for reference, shows the individual PL emission peaks for the C6-doped nanofiber at 492 nm and the LR305-doped nanofiber at 590 nm. Insets are respective microscope images of the nanofibers. It can be seen that the C6-doped nanofiber emits green light while the LR305-doped nanofiber emits red light.

For analysis of the time-dependent light emission at different positions, spectrum tests were conducted along a C6-LR305-codoped nanofiber with a diameter of 450 nm by launching the 473-nm blue light into the nanofiber through the tapered fiber with $P_{ex} \approx 4$ μW. Figure 4(a) shows a coupling junction between a 300 nm diamter tip-sized tapered fiber and the 450 nm diameter C6-LR305-codoped nanofiber. Inset I of Fig. 4(a) shows the closed-up view of the coupling junction marked. Inset II of Fig. 4(a) schematically shows the coupling angle between the tapered fiber and the nanofiber, defined as γ which was calculated to be 15.8° by $\cos\gamma = \cos\theta \times \cos\beta$, where $\theta = 15°$ is the angle between the tapered fiber and the nanofiber measured from the microscope image while $\beta = 5°$ is the attack angle between the tapered fiber and the horizontal line. The reason for forming the angle of 15.8° is for easy to distinguish the fiber tip and the nanofiber. For later characterization, two regions along the nanofiber are marked as white dash boxes A and B, while the two output ends on the left and right of the nanofiber are marked as white dash boxes L and R, respectively.

By launching the 473-nm blue light into the codoped nanofiber through the tapered fiber with $P_{ex} \approx 4$ μW, green light was emitted in the nanofiber as shown in Fig. 4(b). Here, it should be noted that, the coupling efficiency is related to the coupling angle γ between the tapered fiber and the nanofiber and it is estimated to be 30% with $\gamma = 15.8°$[21], so the actual optical power P_{in} coupled into the codoped nanofiber was estimated to be 1.2 μW. In the figure, it is clear that light emission in the region B is much brighter than that in the region A. This can be explained as follows. On condition that the absorption coefficient α stays a constant, the absorption of the excitation light along the PNF obeys an exponential decay as a function of propagation distance by the Beer-Lambert law $I = I_0\exp(-\alpha d)$, where I_0 is the initial input excitation intensity, I is the excitation intensity after a propagation distance of d. The decline in absorption of the excitation light results in the decay of the emitted light along the nanowire. Two bright output spots were also observed at L and R. After 23 minutes excitation by the launched 473-nm blue light (Fig. 4(c)), the region A still remained green while the region B turned red, which indicates that the C6 (emission peak: 492 nm) was emitted stronger in the region A. In other words, the LR305 (emission peak: 590 nm) emitted stronger in the region B. After 57 minutes, the emitted light in all regions became red (Fig. 4(d)). It can be seen that, the output light in the output end L changes from green (Fig. 4(b)) to mix of red and blue, indicating that after 57 min excitation, less and less 473-nm blue light was absorbed. The light spot in the output end R changes from green ($t = 0$) to red ($t = 23$ min), this can be explained as follows. Firstly, the C6 absorbed much more 473-nm light than LR305 at $t = 0$, and emits green. At $t = 23$ min, C6 in region B suffers a decrease in absorbance at 473 nm. Therefore LR305 in region B is able to

absorber more 473-nm light and emits stronger red light. Thus a red spot was observed. From the above description, it can be concluded that the light emission from the codoped nanofiber is a function of both time and position. The former is owing to the decrease of absorbance at 473 nm induced by the photobleaching of dyes while the latter is induced by diverse photobleaching rates along the codoped nanofiber. Since the optical power of excitation light attenuates when guided along the nanofibers, the photobleaching rate is also a function of position and presents a decreasing trend along the nanofiber.

Figure 4(e) shows spectra of the time-dependent PL of the excited polymer nanofiber at t = 0, 23, 57 min. The PL spectra were taken focusing on the middle of the excitation segment (shown as a white cross in the insets of Fig. 4(e)) with a sampling window of 5 × 5 μm^2 via the micro-spectrophotometer. The black curve shows a spectrum with a major emission peak at 492 nm with intensity ratio (IR) at the wavelength of 590 nm (0.3) to 492 nm (1.0) is 0.3, indicating 3 times brighter fluorescence of C6 than LR305 molecules. Therefore the excited segment appears green. Similar analysis can also be applied to the green and red curves, representing the spectrum at t = 23 min and t = 57 min, respectively. The turning of the emission color from green to red

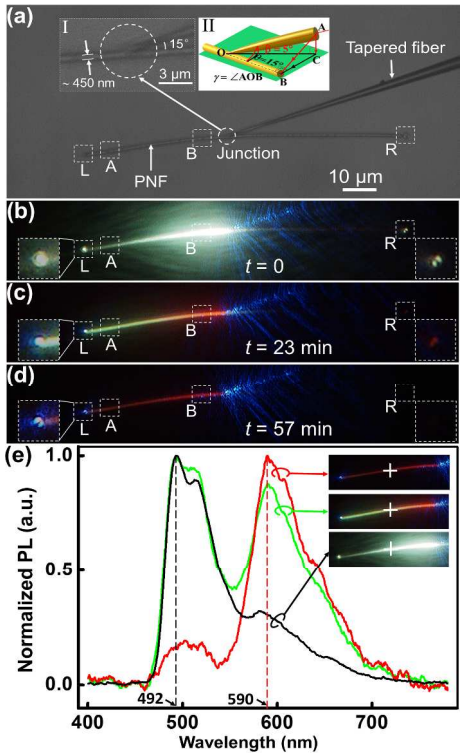

Fig. 4 (a) Optical microscope image of coupling between a tapered fiber and a C6-LR305-codoped polymer nanofiber (diameter ≈ 450 nm, length ≈ 95 μm). Inset I is the closed-up view of the coupling junction. Inset II is the schematic of the calculation of coupling angle. (b–d) PL microscope images of the polymer nanofiber at t = 0, 23, and 57 min, respectively excited by 473 nm blue light with P_{ex} ≈ 4 μW. (e) Normalized PL spectra of the polymer nanofiber shown in (b–d), as quantification of the time-dependent color changing. For instance, black line: excitation time t = 0, showing stronger PL at 492 nm than 590 nm, resulting in green color of the polymer nanofiber in (b). Insets: corresponding microscope images. White cross in the insets: focusing position for spectrum measurement. The microscope images were captured without filters in order to see details about excitation and the 473-nm blue light at the output end on the left.

can be ascribed to the IR varying from 0.3 to 5.0 after excitation of 57 mins.

To show the difference of the light emission in the C6-LR305-codoped polymer nanofibers and macroscopic samples (films), another experiment on the C6-LR305-codoped polymer film has been performed (See Figure S3 in the Supplementary Information). The result shows that, after 57 minutes excitation, the maximum emission intensity at 492 nm decreases only 6.0% in the film while it decreases 87.0% in the nanofiber (Fig. 4(e)), which indicates that the photobleaching rate of C6 is much improved (at least 14 times) in the form of a nanofiber. This is mainly because the surface-to-volume ratio of the nanofiber is larger than that of the film, which can lead to more exposure to the ambient air and thus result in intensify of the photooxidation of dyes. Thus, the photobleaching of the fluorescent dyes is also related to the form of the samples.

Conclusion

Time-pendent light emission at different positions of C6-LR305-codoped polymer nanofibers has been demonstrated. Via continuous waveguiding excitation, the C6-LR305-codoped polymer nanofiber emitted time-dependently at a certain position, from green color with a major peak at 492 nm to red color with a major peak at 590 nm. Time-dependent evolution of light emission varies at different rates at different positions along the polymer nanofiber. Light emission at positions with shorter propagation distance of excitation light is faster due to the variance of photobleaching at different positions along the polymer nanofiber.

Acknowledgement

This work was supported by the National Natural Science Foundation of China (No. 11274395) and the Program for Changjiang Scholars and Innovative Research Team in University (IRT13042).

Notes and References

State Key Laboratory of Optoelectronic Materials and Technologies, School of Physics and Engineering, Sun Yat-Sen University, Guangzhou, 510275, People's Republic of China. E-mail: B.L. (stslbj@mail.sysu.edu.cn); Fax: +86-20-8411 2260; Tel: +86-20-8411 0200

1. I. Cucchi, F. Spano, U. Giovanella, M. Catellani, A. Varesano, G. Calzaferri and C. Botta, *Small,* 2007, **3**, 305–309.
2. F. X. Gu, H. K. Yu, P. Wang, Z. Y. Yang, and L. M. Tong, *ACS Nano*., 2010, **4**, 5332–5338.
3. Y. Ishii, R. Kaminose, and M. Fukuda, *Mater. Lett.,* 2013, **108**, 270–272.
4. Q. H. Song, L. Y. Liu, and L. Xu, *J. Lightwave Technol.*, 2009, **27**, 4374-4376.
5. A. Camposeo, F. Di Benedetto, R. Stabile, A. A. R. Neves, R. Cingolani, and D. Pisignano, *Small,* 2009, **5**, 562-566.
6. Y. Ner, J. G. Grote, J. A. Stuart, and G. A. Sotzing, *Angew. Chem. Int. Ed.*, 2009, **48**, 5134-5138.
7. V. Vohra, G. Calzaferri, S. Destri, M. Pasini, W. Porzio, and C. Botta, *ACS Nano* , 2010, **4**, 1409-1416.
8. C. Giansante, G. Raffy, C. Schäfer, H. Rahma, M. T. Kao, A. G. L. Olive, and A. D. Guerzo, *J. Am. Chem. Soc.,* 2011, **133**, 316-325.
9. C. Giansante, C. Schäfer, G. Raffy, and A. D. Guerzo, *J. Phys. Chem. C*, 2012, **116**, 21706-21716.

10. X. S. Xie, and J. K. Trautman, *Annu. Rev. Phys. Chem.,* 1998, **49**, 441–480.
11. C. Eggeling, J. Widengren, R. Rigler, and C. A. M. Seidel, *Anal. Chem.,* 1998, **70**, 2651-2659.
12. M. Wang, R. Holmes-Davis, Z. Rafinski, B. Jedrzejewska, K. Y. Choi, M. Zwick, C. Bupp, A. Izmailov, J. Paczkowski, B. Warner, and H. Koshinsky, *Anal. Chem.,* 2009, **81**, 2043–2052.
13. C. Maibohm, J. R. Brewer, H. Sturm, F. Balzer, and H.-G. Rubahn, *J. Appl. Phys.,* 2006*,* **100**, 054304.
14. A. Camposeo, F. Di Benedetto, R. Stabile, R. Cingolani and D. Pisignano, *Appl. Phys. Lett.*,2007, **90**, 143115.
15. R. Zondervan, F. Kulzer, M. A. Kol'chenko, and M. Orrit, *J. Phys. Chem. A*, 2004, **108**, 1657-1665.
16. G. Gupta, W. H. Steier, Y. Liao, J. D. Luo, L. R. Dalton, and A. K.-Y. Jen, *J. Phys. Chem. C*, 2008, **112**, 8051–8060.
17. B. Piccione, L. K. van Vugt, and R. Agarwal, *Nano Lett.*, 2010, **10**, 2251–2256.
18. F. Di Benedetto, A. Camposeo, S. Pagliara, E. Mele, L. Persano, R. Stabile, R. Cingolani, and D. Pisignano, *Nat. Nanotechnol.*, 2008, **3**, 614–619.
19. K. Takazawa, J. Inoue, and K. Mitsuishi, *Nanoscale*, 2014, **6**, 4174–4181.
20. R. Zhang, H. Q. Yu, and B. J. Li, *Nanoscale,* 2012, **4**, 5856-5859.
21. W. He, B. J. Li, and E. Y. B. Pun, *Opt. Lett.,* 2009, **34**, 1597-1599.